

Heat and mass transfer analysis of Brinkman type fractional nanofluid over a vertical porous plate with velocity slip and Newtonian heating

Aneela Razzaq

Department of Mathematics, University of the Punjab, Lahore, Pakistan.
Email: aneelaimranphds@gmail.com

Nauman Raza

Department of Mathematics, University of the Punjab, Lahore, Pakistan.
Email: nauman.math@pu.edu.pk

Received: 07 February, 2019 / Accepted: 17 April, 2019 / Published online: 01 August, 2019

Abstract. The partial differential equations of integer order describes only the models of classical nanofluids and do not consider the memory effects. For the description of the influence of memory on the nanofluids, differential equations with non-integer derivatives are used for the modeling of fractional nanofluids. This investigation explores the unsteady mixed convection fractional nanofluids flow of Brinkman type near a plate placed vertically in a permeable medium. Mass and heat transfer investigation is carried out under the thermal and chemical reaction effects. Four different nanoparticles named Silver (Ag), Aluminium Oxide (Al_2O_3), Copper (Cu), Titanium Oxide (TiO_2) are dispersed in water which is a base fluid. The modeled system of partial differential equations are transformed into dimensional form through suitable dimensionless variables. By using Laplace transformation, the semi analytic solutions for velocity, temperature and concentrations field are developed. Then by using MATHCAD, inverse Laplace transform has been computed numerically. The acquired solutions meet all imposed initial and boundary conditions and change to similar solutions for ordinary nanofluid when fractional parameter value is taken as one. Influence of distinct physical parameters such as Brinkman parameter, fractional parameter, radiation parameter and volume fraction on the velocity, temperature and concentration profiles are shown through graphs. The tables for Sherwood number, Nusselt number are also calculated for different values of emerging parameters. The major result of our study is ordinary nanofluid flow is decelerator than the fractional nanofluid. Also, the fractional parameter has strong influence over heat transfer phenomena. It is also explored in this study that heat transfer rate is high for fractional nanofluid as compared to ordinary nanofluid.

AMS (MOS) Subject Classification Codes: 76A10**Key Words:** Brinkman fluid; Velocity field; Nanoparticles.**Nomenclature**

h'	fluid velocity component (ms^{-1})
C	concentration
ψ	porous media
g	acceleration due to gravity (ms^{-2})
γ_1	heat transfer coefficient ($WK^{-1}m^{-2}$)
k_1	permeability of the porous media
β	material parameter of the Brinkman fluid
q_r	radiative flux
k_2	chemical reaction parameter
ρ'_{nf}	density of nanofluid (kgm^{-3})
μ'_{nf}	dynamic viscosity of nanofluid ($kgm^{-2}s^{-1}$)
σ'_{nf}	electrical conductivity of nanofluid ($s^3A^2kg^{-1}m^{-3}$)
$(\beta_T)_{nf}$	thermal expansion coefficient of nanofluid
$(\beta_C)_{nf}$	concentration coefficient of nanofluid
$(\rho C_p)'_{nf}$	specific heat capacity of nanofluid
k'_{nf}	thermal conductivity of nanofluid
ϑ	volume fraction of nano particle
T_∞	constant temperature (K)
C_∞	constant concentration
B_0	applied magnetic field ($Kgs^{-2}A^{-1}$) C_p
C_p	specific heat at constant pressure
ρ'_f	density of base fluid (Kgm^{-3})
Re	Reynold number
β_1	Brinkman parameter in dimensionless form
M	magnetic parameter
Gr	thermal Grashof number
Gm	mass Grashof number
Pr	Prandtl number
Sc	Schmidt number
Nr	radiation parameter
χ	dimensionless chemical reaction parameter
α	fractional parameter
s	Laplace parameter

1. INTRODUCTION

During the last few decades, the study of non-Newtonian fluids has become an active research area because of its extensive utilization in chemical engineering, pharmaceutical industry and cosmetics [1, 36]. In literature, there are enormous models concerning with non-Newtonian fluids. One of the most important model is the Brinkman's type

fluid model. The viscous fluid model past through a porous body has been firstly introduced by Darcy [9]. His theory is known as Darcy's law that describes the fluid flow through porous surfaces with low permeability. However, the flow over highly porous bodies does not follow the Darcy's law. For these type of fluid flows over high porous surfaces [5, 45], Brinkman's model is applicable. Brinkman's type fluid is a viscous fluid of constant density that describes flow over highly penetrable surface. Very few investigations have been reported in this field, concerning Brinkman's type fluids. Specially, convective heat transfer of Brinkman's type fluids also along with mass transfer effects are less explored, although such issues have enormous implementations in engineering and industry [14, 15, 28, 37, 72]. Low value of thermal conductivity of various fluids for instance: water, oil and ethylene glycol have a serious limitations in enhancing the compactness and performance of many engineering equipment such as electrical devices and heat exchangers. In order to overcome these difficulties, there is a strong demand to discover those fluids which have higher value of heat conductivity. Hence, various techniques had developed to enhance the heat transfer rate in various engineering tools. The heat conductivity can be increased by staying solid particles in base fluids. These solid particles are named as nanoparticles and fluids are termed as nanofluids. There are different shapes of nanoparticles like cylindrical, spherical and bricks etc. Also, the shape of nanoparticles has a very important role for strengthening the heat transfer measure. In this field, the pioneer work has been done by Choi [8]. He enhances the thermal conductivity of fluids with the use of nanoparticles made up of metals *Al*, *Cu* due to their greater thermal conductivity. Nanoparticles have enormous applications in field of ultrasonic display, compressional wave and shear wave [17]. For nanofluid flows, some important investigations have been done by famous researchers in [22, 23, 24, 25, 29, 33, 62]. Convection nanofluid flows under the effect of radiation have been investigated along an infinite vertical plate by Loganathan *et al.* [35]. Ansari *et al.* [64] studied the MHD convection flow under the combined effect of radiation and rotation with ramped wall temperature in porous media. They considered the flow pass across the vertical plate which is impulsively moving. Akber *et al.* [3] discussed the hydromagnetic stagnation point flow with convective boundary conditions. Ibrahim *et al.* [20] explored heat transfer and radiation effects over a stretchable sheet which is non-linear. Anwar *et al.* [4] considered the conjugate effects of heat and mass transfer for nanofluid over a nonlinear stretchable sheet. For the rotating system, Sheikholeslami and Ganji *et al.* [65] studied the three dimensional MHD flow of nanofluids with heat and mass transfer. Furthermore, the combined phenomena of chemical reaction with mass transfer has become an important research area such as in gas liquid system. Chemical reactions are of two types for example heterogeneous or homogeneous. First order chemical reaction is defined as direct relation between order of chemical reaction and concentration of chemical reaction. In various chemical engineering phenomena, first order chemical reaction has been used widely [11]. Rashad *et al.* [59] investigated the impact of chemical reaction on heat and mass transfer by mixed convection flow through a sphere in a porous medium. Hayat *et al.* [21] explored the heat and mass transfer analysis for second grade fluid in the presence of chemical reaction.

For explaining the viscoelastic behavior of fluid models, fractional approach has been successfully utilized by different researchers in recent years. In this approach, ordinary time

derivatives are replaced by fractional order time derivative. Fractional calculus has wide-spread applications not only in physics and fluid dynamics but also in other basic sciences such as chemistry, biology, rheology and geology. In this regard, the pioneer work has been done by Garaham [19] in which he successfully employed the use of fractional derivative for the explanation of viscoelasticity. Liu *et al.* [6] discussed the Maxwell nanofluid fractional model near a moving plate. Later on, Liu *et al.* [46] modeled the fractional nanofluid with stagnation point flow. Fetecau *et al* [16]. considered the convection flow of fractional nanofluid over a vertical isothermal plate with radiation effects in which they exactly solved the problem via Laplace transform.

The no-slip boundary condition is not sufficient for the description of many fluid problems for instance in thin fluid mechanics, multiple interface problems, wavy tubes flow, flows in micro channels [66], therefore, it is necessary to consider the slip effects as it has found enormous applications in industry and engineering. The main causes for the production of slip over a surface are fluid rarefaction, velocity of fluid and surface roughness. Navier [44] introduced slip boundary condition in which he proposed the relation between fluid velocity and shear stress. A large number of slip models have been shown in [7, 10, 39, 40, 54]. Later on, Ilyas [34] discussed the MHD slip flow of nanofluid with MoS_2 as nanoparticle for porous medium. He used the perturbation technique in his study. Kandasamy *et al.* [32] studied the SWCNTS-nanofluid flow under the slip effects and chemical reaction. They numerically solved the problem with RK-4 method along with shooting technique. Ghoshdastidar [18] worked on distinct lines of practical applications for example, transfer of heat in pipes and lines, conduction of heat from electronic appliances, heat transfer from heat exchanger and electrical heater. Free convection problems are mostly formulated under various situations like ramped wall temperature, constant temperature of surface and surface heat flux. In some problems, when the above postulates are failed, we take the condition termed as Newtonian heating in which the rate of heat transfer from the surrounding surface with finite heat is proportional to the local temperature of surface. However, because of diversity of practical applications, the Newtonian heating appears in various engineering appliances such as double pipe heat exchanger, heat transfer from fins and cooling of engine. The Newtonian heating concept was presented firstly by Markin [38]. The most recent results in this field are Narahari [42], Narahari and Dutta [43] and Ramzan *et al.* [56].

EI-Kabeir and Rashad *et al.* [12] analyzed the heat transfer in the boundary layer flow on a circular cylinder in the nanofluid. Later on, Rashad *et al.* [57] discussed mixed convection flow of non-Newtonian fluid from a vertical surface filled with nanofluid using finite difference method. Chamkha *et al.* [41] investigated the free convection flow along a plate located vertically for nanofluid filled with porous medium which is non-Darcy. They used the modified iterative scheme in this study. Rashad *et al.* [58] explored mixed convection problem of nanofluid flowing along circular cylinder emerged using the convective conditions. Rashad *et al.* [13] studied the thermal radiation effects on nanofluid flow about a solid sphere in a porous medium. Zahar *et al.* [71] modeled the boundary layer flow under the high suction effects through a singular perturbation technique. Rashad *et al.* [60] analysed the MHD Ferrofluid model along a wedge under the composite effects of partial slip and heat radiation.

Usman *et al.* [68] worked on Casson nanofluid with velocity and thermal slip effects by using the collocation method. Later on, Usman *et al.* [69] found the wavelets solution of MHD fluid flow for three dimensions under the combined effects of slip and thermal radiations. Rizwan Ul Haq *et al.* [26] worked on MHD convection flow in a porous cavity. Later on, Rizwan Ul Haq *et al.* [27] worked on heat transfer study of Cu-water fluid flow in the rhombus. Purusothaman *et al.* [47] studied the numerical analysis of natural convection cooling process in three dimensions. The enclosure is filled with nanofluid with Copper and Aluminium as nanoparticles. They used the finite element method in their study. Purusothaman *et al.* [48] investigated the numerical analysis of heat transfer and 3D natural convection in a cubical cavity. Later on, natural convection in cubical shaped cavity under the action of heat transfer had been examined by Purusothaman *et al.* [49]. Purusothaman *et al.* [50] carried out the numerical investigation in 3D-enclosure filled with Cu-nanoparticles by taking two different base fluids. Purusothaman [51] investigated the natural convection through porous media with heat transfer effects by using the nanofluid. Purusothaman *et al.* [52] considered simultaneously the vibration and magnetic effects on a second grade fluid through the porous module. Rahimi *et al.* [55] carried out the investigation of 3D-natural convection with entropy generation in a cuboid with Cu-nanofluid by considering water as base fluid. They solved the problem by using two models. Purusothaman and Malekshah [53] studied numerically the magnetohydrodynamic free convection nanofluid flow.

Wahab *et al.* [70] explored the nanofluid flow problem over a stretching sheet under the action of slip condition and Joule heating effect. Ishaq *et al.* [31] worked on MHD flow of Eyring power nanofluid over a porous sheet which is stretching. Hussain *et al.* [30] solved the bioconvection model between two parallel plates under the action of heat and mass transfer effects of squeezing nanofluid flow. Raza [61] explained the fractional rotational flow of unsteady second grade fluid. Farhad *et al.* [2] examine the MHD flow of nanofluids of Brinkman type under combined effects of heat and mass transfer for the porous media with four different types of spherical shaped nanoparticles. They used the Laplace transform technique.

Here, we extend the work of Farhad *et al.* [2] by using the fractional derivatives in his model and changing the boundary conditions. The semi-analytic solutions for velocity profile are obtained with the aid of Laplace transformation for fractional calculus. Inverse Laplace transformation has been computed numerically with the aid of MATHCAD and further two numerical algorithms named Stehfest's algorithm [63] and Tzou' algorithm [67] for the comparison of results. The velocity, temperature and concentration results are developed and shown through graphs with related discussion and concluding remarks.

2. PROBLEM CONSTRUCTION

Let us consider an incompressible unsteady Brinkman nanofluid model near a semi infinitely plate located in the (x, z) plane of cartesian coordinate system x, y, z . The plate is placed vertically in the permeable surrounding. The fluid flow is imposed to the impact of magnetic field B_0 which is applied constantly in the transverse direction to the fluid flow. The induced magnetic field in this case can be neglected by choosing the small value of magnetic Reynold number. The simultaneous heat and mass transfer analysis is considered under the influence of radiation and chemical reaction of first order. Let T_∞ and C_∞ are

the constant temperature and constant concentration of fluid and plate which are initially at rest. whereas time t increased from zero, the plate begins to move in its plane with velocity in x -direction. The temperature and concentration of plate are changed linearly with time and take constant value thereafter. Figure 1 explains the geometry of the problem and the related coordinate system.

The fluid velocity in this problem is

$$H = H(y_1, t_1) = h'(y_1, t_1)i, \quad (2.1)$$

whereas \vec{i} is unit vector along x -direction. Under above stated assumptions, the governing modeled equations [66] are as under:

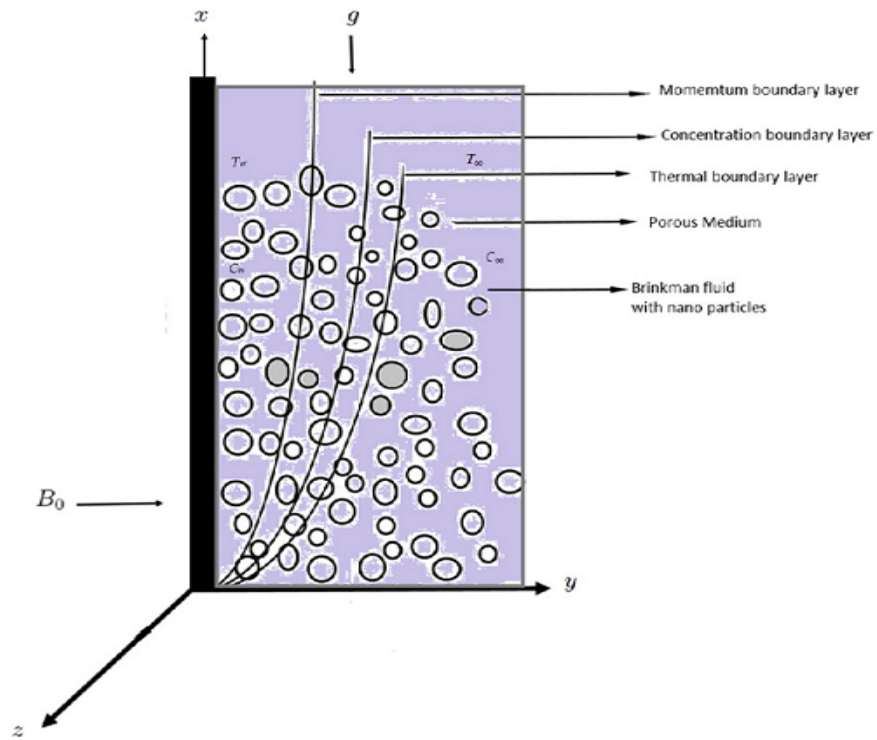


Figure 1

$$\rho'_{nf} \left(\frac{\partial h'}{\partial t_1} + \beta h' \right) = \mu_{nf} \frac{\partial^2 h'}{\partial y_1^2} - \left(\sigma'_{nf} B_0^2 + \frac{\mu_{nf} \psi}{k_1} \right) h' + g(\rho\beta_T)'_{nf} (T - T_\infty) + g(\rho\beta_C)'_{nf} (C - C_\infty), \quad (2.2)$$

$$(\rho c_p)'_{nf} \frac{\partial T}{\partial t_1} = k'_{1nf} \frac{\partial^2 T}{\partial y_1^2} - \frac{\partial q_r}{\partial y_1}, \quad (2.3)$$

$$\frac{\partial \mathcal{C}}{\partial t_1} = D_{nf} \frac{\partial^2 \mathcal{C}}{\partial y_1^2} - k_2(\mathcal{C} - \mathcal{C}_\infty), \quad (2.4)$$

subject to initial along with boundary constraints:

$$h'(y_1, 0) = 0, \quad T(y_1, 0) = \mathcal{T}_\infty, \quad \mathcal{C}(y_1, 0) = \mathcal{C}_\infty, \quad (2.5)$$

$$h'(0, t_1) - b \frac{\partial h'(0, t_1)}{\partial y_1} = U_0 H(t) \cos \omega t_1, \quad \frac{\partial T(0, t_1)}{\partial y_1} = -\gamma_1 T(0, t_1), \quad (2.6)$$

$$\mathcal{C}(0, t_1) = \mathcal{C}_w,$$

$$h'(y_1, t_1) \rightarrow 0, \quad T(y_1, t_1) \rightarrow \mathcal{T}_\infty, \quad \mathcal{C}(y_1, t_1) \rightarrow \mathcal{C}_\infty, \quad y_1 \rightarrow \infty, \quad (2.7)$$

Here h' , T , \mathcal{C} , ψ , g and γ_1 represents fluid velocity, temperature, concentration, porous media, acceleration caused by gravity and heat transfer co-efficient respectively. Also, k_1 denotes the penetrability of media having pores, β shows the material variable of Brinkman fluid, q_r represents the radiative flux and k_2 is parameter of chemical reaction. Futhermore, ρ'_{nf} , μ'_{nf} , σ'_{nf} , $(\beta_T)'_{nf}$, $(\beta_C)'_{nf}$, $(\rho C_p)'_{nf}$ and k'_{1nf} are the density, dynamic viscosity, electrical conductivity, thermal expansion co-efficient, concentration co-efficient, specific heat capacity and thermal conductivity of nanofluids. The expressions for nanofluids are:

$$\mu'_{nf} = \frac{\mu_f}{(1 - \vartheta)^{2.5}}, \quad (2.8)$$

$$(\rho \beta_T)'_{nf} = (1 - \vartheta)(\rho \beta_T)'_f + \vartheta(\rho \beta_T)'_s, \quad (2.9)$$

$$(\rho \beta_C)'_{nf} = (1 - \vartheta)(\rho \beta_C)'_f + \vartheta(\rho \beta_C)'_s, \quad (2.10)$$

$$\rho'_{nf} = (1 - \vartheta)\rho'_f + \vartheta\rho'_s, \quad (2.11)$$

$$(\rho C_p)'_{nf} = (1 - \vartheta)(\rho C_p)'_f + \vartheta(\rho C_p)'_s, \quad (2.12)$$

$$\sigma'_{nf} = \sigma'_f \left(1 + \frac{3(\sigma' - 1)\vartheta}{(\sigma' + 2) - (\sigma' - 1)\vartheta}\right), \quad (2.13)$$

$$\sigma' = \frac{\sigma'_f}{\sigma'_s}, \quad (2.14)$$

$$\frac{k'_{1nf}}{k'_f} = \frac{(k'_s + 2k'_f) - 2\vartheta(k'_f - k'_s)}{(k'_s + 2k'_f) + \vartheta(k'_f - k'_s)}, \quad (2.15)$$

where as ϑ , C_p , ρ'_f stands for volume fraction of nanoparticles, specific heat at constant pressure and density of base fluid respectively. The above declaration in equations (8)-(15) are used for only spherical shaped nanoparticles. The readers can refer to Table 1 [17] for different shapes of nanoparticles with different values of dynamic viscosity and thermal conductivity. The Rosseland approximation of radiative heat flux is given by:

$$q_r = \frac{-4\sigma_1}{3k_3} \frac{\partial T^4}{\partial y}, \quad (2.16)$$

where σ_1 and k_3 are the Stefan-Boltzman constant and mean absorption co-efficient. T^4 is linearized with Taylor series and omitting second and higher terms, we get:

$$\mathcal{T}^4 = 4\mathcal{T}\mathcal{T}_\infty^3 - 3\mathcal{T}_\infty^4. \quad (2. 17)$$

The dimensionless variables are

$$\hat{h}^* = \frac{h'}{U_0}, \hat{y}^* = \frac{U_0}{v}y_1, \hat{t}^* = \frac{U_0^2}{v}t_1, \theta = \frac{\mathcal{T} - \mathcal{T}_\infty}{\mathcal{T}_\infty}, \phi = \frac{\mathcal{C} - \mathcal{C}_\infty}{\mathcal{C}_w - \mathcal{C}_\infty}, \quad (2. 18)$$

Introducing these into equations (2)-(4), we get:

$$\frac{\partial \hat{h}}{\partial \hat{t}} = \frac{1}{A_1} \frac{\partial^2 \hat{h}}{\partial \hat{y}^2} - H\hat{h} + Gr_0\theta + Gm_0\phi, \quad (2. 19)$$

$$b_0 \frac{\partial \theta}{\partial \hat{t}} = \frac{\partial^2 \theta}{\partial \hat{y}^2}, \quad (2. 20)$$

$$\frac{\partial \phi}{\partial \hat{t}} = \frac{1}{S_c} \frac{\partial^2 \phi}{\partial \hat{y}^2} - \chi\phi. \quad (2. 21)$$

The transformed initial along with boundary specifications:

$$\hat{h}(\hat{y}, 0) = 0, \theta(\hat{y}, 0) = 0, \phi(\hat{y}, 0) = 0, \quad (2. 22)$$

$$\hat{h}(0, \hat{t}) - b \frac{\partial \hat{h}(0, \hat{t})}{\partial \hat{y}} = H(\hat{t}) \cos \omega \hat{t}, \quad \frac{\partial \theta(0, \hat{t})}{\partial \hat{y}} = -\gamma[\theta(0, \hat{t}) + 1], \quad \phi(0, \hat{t}) = 1, \quad (2. 23)$$

$$\hat{h}(\hat{y}, \hat{t}) \rightarrow 0, \theta(\hat{y}, \hat{t}) \rightarrow 0, \phi(\hat{y}, \hat{t}) \rightarrow 0 \text{ as } \hat{y} \rightarrow \infty. \quad (2. 24)$$

Table 1: Thermophysical properties of nanofluids

	$\rho(kg/m^3)$	$c_p(1/kgK)$	$k(W/mK)$	$\beta \times 10^{-5}(1/K)$
H_2O	997.10	4179.0	0.6130	21.0
Al_2O_3	3970.0	765.0	40.0	0.850
Cu	8933.0	385.0	401.0	1.670
TiO_2	4250.0	6862.0	8.9528	0.90
Ag	10.500	235.0	429.0	1.890

where

$$A_1 = (1 - \vartheta)^{2.5}[(1 - \vartheta) + \vartheta(\frac{\rho'_s}{\rho'_f})], H = M + \frac{1}{K} + \beta_1, \quad (2. 25)$$

$$Gr_0 = \vartheta_2 Gr, Gm_0 = \vartheta_3 Gm, b_0 = \frac{Pr\vartheta_4}{\lambda_{nf}(1 + Nr)}, \quad (2. 26)$$

$$\vartheta_1 = 1 + \frac{3(\sigma' - 1)\vartheta}{(\sigma' + 2) - (\sigma' - 1)\vartheta}, \vartheta_2 = \frac{(1 - \vartheta)\rho'_f - \vartheta\rho'_s(\frac{\beta_{Tf}}{\beta_{Ts}})}{\rho'_{nf}}, \quad (2. 27)$$

$$\vartheta_3 = \frac{(1 - \vartheta)\rho'_f - \vartheta\rho'_s(\frac{\beta_{cs}}{\beta_{cs}})}{\rho'_{nf}}, \vartheta_4 = (1 - \vartheta) + \vartheta\frac{(\rho c_p)'_s}{(\rho c_p)'_f}, \lambda_{nf} = \frac{k'_{1nf}}{k'_{1f}}, \quad (2. 28)$$

where $\beta_1 = \frac{\beta\nu}{U_0^2}$ is the Brinkman parameter in dimensionless form, $M = \frac{\vartheta_1\nu\sigma'_f B_0^2}{\rho'_{nf} U_0^2}$ represents the magnetic parameter, $\gamma = \frac{\gamma_1\nu}{U_0}$ is the Newtonian heating parameter. The permeability of porous medium is $\frac{1}{K} = \frac{\nu_{nf}\vartheta\nu}{kU_0^2}$. $Gr = \frac{\nu_g\beta_{Tf}(T_w - T_\infty)}{U_0^3}$ and $Gm = \frac{\nu_g\beta_{Cf}(C_w - C_\infty)}{U_0^3}$ are the thermal Grashof number and mass Grashof number respectively. $Pr = \frac{(\mu c_p)'_f}{k'_{1f}}$, $Sc = \frac{\nu}{D_{nf}}$, $Nr = \frac{16\sigma_1 T_\infty^3}{3k_{1nf}k_a}$, $\chi = \frac{k_2\nu}{U_0^2}$ are Prandtl number, Schmidt number, radiation parameter and chemical reaction parameter respectively.

The fractional nano fluid model is given by the fractional differential equations:

$$\mathcal{D}_{\hat{t}}^\alpha \hat{h}(\hat{y}, \hat{t}) = \frac{1}{A_1} \frac{\partial^2 \hat{h}(\hat{y}, \hat{t})}{\partial \hat{y}^2} - H\hat{h}(\hat{y}, \hat{t}) + Gr_0\theta(\hat{y}, \hat{t}) + Gm_0\phi(\hat{y}, \hat{t}), \quad (2. 29)$$

$$b_0 \mathcal{D}_{\hat{t}}^\alpha \theta(\hat{y}, \hat{t}) = \frac{\partial^2 \theta(\hat{y}, \hat{t})}{\partial \hat{y}^2}, \quad (2. 30)$$

$$\mathcal{D}_{\hat{t}}^\alpha \phi(\hat{y}, \hat{t}) = \frac{1}{S_c} \frac{\partial^2 \phi(\hat{y}, \hat{t})}{\partial \hat{y}^2} - \chi\phi(\hat{y}, \hat{t}), \quad (2. 31)$$

together with the conditions given in equations (22)-(24). The operator $\mathcal{D}_{\hat{t}}^\alpha$ shows Caputo fractional derivative with respect to time is described as:

$$\mathcal{D}_{\hat{t}}^\alpha \hat{h}(\hat{y}, \hat{t}) = \begin{cases} \frac{1}{\Gamma(1-\alpha)} \int_0^{\hat{t}} \frac{1}{(\hat{t}-s')^\alpha} \frac{\partial u(\hat{y}, s')}{\partial s'} ds', & 0 \leq \alpha < 1, \\ \frac{\partial \hat{h}(\hat{y}, \hat{t})}{\partial \hat{t}}, & \alpha = 1. \end{cases} \quad (2. 32)$$

3. SOLUTION OF THE PROBLEM

3.1. Calculation of temperature field. Taking Laplace transformation of equation (30) and considering the related initial as well as boundary conditions, we reached at

$$b_0 s^\alpha \theta(\hat{y}, s) = \frac{\partial^2 \theta(\hat{y}, s)}{\partial \hat{y}^2}, \quad (3. 33)$$

where s is transformation variable. The Laplace transformation $\theta(\hat{y}, s)$ of $\theta(\hat{y}, \bar{t})$ should meet the required specifications:

$$\frac{\partial \theta(0, s)}{\partial \hat{y}} = -[\theta(0, s) + \frac{1}{s}], \theta(\infty, s) = 0. \quad (3. 34)$$

The solution of the problem (33) and (34) is

$$\theta(\hat{y}, s) = \frac{-1}{s(1 - \sqrt{b_0 s^\alpha})} e^{-\sqrt{b_0 s^\alpha} \hat{y}}. \quad (3. 35)$$

3.2. Calculation of concentration field. Taking Laplace transform of equation (31) and considering the related initial along with boundary conditions, we evaluate at

$$s^\alpha \phi(\hat{y}, s) = \frac{1}{S_c} \frac{\partial^2 \phi(\hat{y}, s)}{\partial \xi^2} - \chi \phi(\hat{y}, s), \quad (3.36)$$

where the Laplace transformation $\phi(\hat{y}, s)$ of $\phi(\hat{y}, \hat{t})$ should meet the required conditions:

$$\phi(0, s) = \frac{1}{s}, \quad \phi(\infty, s) = 0. \quad (3.37)$$

The Laplace solution to the problem (36) and (37) is

$$\phi(\hat{y}, s) = \frac{1}{s} e^{-\sqrt{S_c(s^\alpha + \chi)} \hat{y}}. \quad (3.38)$$

3.3. Calculation of velocity function. By taking Laplace transformation to equation (29) and considering related initial along with boundary conditions, we arrived at

$$s^\alpha \hat{h}(\hat{y}, s) = \frac{1}{A_1} \frac{\partial^2 \hat{h}(\hat{y}, s)}{\partial \hat{y}^2} - H \hat{h}(\hat{y}, s) + Gr_0 \theta(\bar{y}, s) + Gm_0 \phi(\hat{y}, s), \quad (3.39)$$

where Laplace transformation $\hat{h}(\hat{y}, s)$ of $\hat{h}(\hat{y}, \hat{t})$ should meet required conditions:

$$\hat{h}(0, s) - b \frac{\partial \hat{h}(0, s)}{\partial \hat{y}} = \frac{s}{s^2 + w^2}, \quad \hat{h}(\infty, s) = 0. \quad (3.40)$$

The solution of the problem (39) and (40) is

$$\begin{aligned} \hat{h}(\hat{y}, s) = c_2 e^{-\sqrt{A_1(s^\alpha + H)} \hat{y}} + \frac{A_1 Gr_0}{s(b_0 s^\alpha - A^2)(1 - \sqrt{b_0 s^\alpha})} e^{-\sqrt{b_0 s^\alpha} \hat{y}} \\ - \frac{A_1 Gm_0}{(S_c(s^\alpha + \chi) - A^2)s} e^{-\sqrt{S_c(s^\alpha + \chi)} \hat{y}}, \end{aligned} \quad (3.41)$$

where c_2 is

$$\begin{aligned} c_2 = \frac{s}{s^2 + w^2} - \frac{A_1 Gr_0 (1 + b\sqrt{b_0 s^\alpha})}{s(b_0 s^\alpha - A^2)(1 - \sqrt{b_0 s^\alpha})} \\ + \frac{A_1 Gm_0 (1 + b\sqrt{S_c(s^\alpha + \chi)})}{(S_c(s^\alpha + \chi) - A^2)s} / 1 + b\sqrt{A_1(s^\alpha + H)}. \end{aligned} \quad (3.42)$$

4. GRAPHICAL DISCUSSION AND RESULTS

For the explanation of the influence of distinct parameters for example β_1 Brinkman parameter, ϕ the volume fraction, Gr Grashof number, Gm modified Grashof number, M magnetic parameter, Pr Prandtl number, Nr radiation parameter, Sc Schmidt number on velocity, temperature and concentration fields, graphs (2-15) are portrayed. Water is chosen as ground fluid and four various nanoparticles (Silver Ag , Copper Cu , Titanium oxide TiO_2 and Aluminium oxide Al_2O_3) of spherical shapes are taken.

Figure 2 explains the behavior of Brinkman parameter β_1 on velocity profile. Since Brinkman parameter is ratio of the drag force to the density, therefore for raising value of β_1 , there is an increase in the drag force which decreases the velocity. It is deduced that Brinkman nanofluid is slower as compared to ordinary nanofluid.

Figure 3 depicts the influence of nanoparticle volume fraction ϕ on velocity function. The range of volume fraction ϕ is $0 \leq \phi \leq 0.04$ because sedimentation occurs when value of ϕ increases 0.08 and the case leads to pure water (base fluid). In this situation, an increase in volume fraction ϕ of nanoparticles means that the increase of particles in the fluid and hence the frictional force increases among particles which results in deceleration of velocity.

Figure 4 highlights the impact of Gr on velocity profile for fractional nanofluids by taking the different value of fractional parameter α . Various values of Gr are selected. Free convection take place when $Gr = 0$ and $Gr > 0$ shows natural convection. It can be seen from this graph that a larger value of Grashof number Gr leads to accelerate the flow of fractional nanofluid. Because physically Gr is the relation between buoyancy force and viscous force. Hence an increment in buoyancy force increases the flow velocity. Figure 5 explains the impact of mass or modified Grashof number Gm on velocity distribution. When $Gm = 0$, there is no convection due to mass transfer. Furthermore, this sketch shows that the buoyancy force increases for larger value of Gm and hence the fluid flow accelerates.

Figure 6 explains changes in velocity function for various Sc (Schmidt number) for fractional nanofluids. It is observed that higher the rate of Schmidt parameter Sc , velocity function decelerates. Since Schmidt number is defined as the ratio of viscous force and mass diffusivity, hence increasing the value of Schmidt number Sc means an increase in viscous force causes to decrease the velocity. Consequently, the effects of magnetic parameter M and Schmidt number Sc on velocity function are similar. The same findings have been observed in [32, 34].

Figure 7 explains that fluid velocity accelerates at larger values of time interval \hat{t} . Figure 8 shows that velocity distribution is directly related to the porosity parameter K . It is due to the reason that raising the permeability value causes a decrease in frictional forces resulting fluid flow move more speedily.

Figure 9 illustrates the effect of radiation parameter Nr on the velocity profile for fractional nanofluid. It is noted that for an increase in Nr , the fluid velocity also increases.

The behavior of magnetic parameter M on the velocity distribution for fractional nanofluid is disclosed in Figure 10. Graph shows that when there is no applied magnetic field, fluid velocity for fractional fluid is considerably high as compared to ordinary nanofluid and it tends to decrease when magnetic field is enhanced. This physical illustration of velocity function shows that higher the value of magnetic factor M generates resistive force named Lorentz force that acts oppositely to fluid flow direction and so causes reduction in fluid velocity of fractional nanofluid due to its resistive nature.

The variations in the temperature field for nanofluid with respect to time interval are portrayed in Figure 11. Figure 11 reveals that the temperature field decreases at different time intervals $\hat{t} = 0.1, 0.04, 2$.

The Figures 12, 13, 14 depicts the changes in the concentration field for fractional nanofluid under the influence of the physical parameters: chemical reaction parameter, Schmidt number and time \hat{t} respectively. At increased value of the chemical reaction parameter tends to enhance the concentration field while a larger value of Schmidt number decays the concentration field. Figure 15 depicts the changes in the skin friction, Nusselt number and Sherwood number for different values of fractional parameter. The skin friction coefficient shows an inverse relation corresponding to fractional parameter. The Prandtl number Pr is

set to be 0.78 through out this study.

For the presentation of numerical results of velocity function, we made use numerical algorithms named Stehfest's [63] as well as Tzou's algorithm [67] and in order to show the comparison with the existing results. With Stehfest's algorithm, the inverse Laplace transform is given by

$$\hat{h}(\hat{y}, t) = \frac{\ln 2}{t} \sum_{k=1}^N V_k \bar{h}\left(\hat{y}, \frac{\ln 2}{t}\right),$$

$$V_k = (-1)^{k+\frac{N}{2}} \sum_{j=\lceil \frac{k+1}{2} \rceil}^{\min(k, \frac{N}{2})} \frac{j^{\frac{N}{2}} 2j!}{(\frac{N}{2}-j)! j! (j-1)! (k-j)! (2j-k)!}, \quad (4.43)$$

where N denotes total number of terms and should be even ($N=16$ for good accuracy). The Tzou's algorithm described Riemann-sum approximation. In this technique, inverse Laplace transform is described as

$$\hat{h}(\hat{y}, t) = \frac{e^{4.7}}{t} \left[\frac{1}{2} \bar{h}\left(\hat{y}, \frac{4.7}{t}\right) + \operatorname{Re} \left(\sum_{k=1}^{N_1} (-1)^k \bar{h}\left(\hat{y}, \frac{4.7 + k\pi i}{t}\right) \right) \right], \quad (4.44)$$

where $\operatorname{Re}(\cdot)$, i and N_1 stands for real, imaginary part and natural number respectively.

Table 2: Distinct values of velocity distribution $\hat{h}(\hat{y}, \hat{t})$ with different values of \hat{y} .

\hat{y}	$\hat{h}(\hat{y}, \hat{t})$ Stehfest's	$\hat{h}(\hat{y}, \hat{t})$ Tzou's
0	00.138555	00.143648
00.1	00.134064	00.139055
00.2	00.129642	00.134597
00.3	00.125294	00.130192
00.4	00.121024	00.125824
00.5	00.116834	00.121503
00.6	00.112728	00.117245
00.7	00.108707	00.113065
00.8	00.104774	00.108972
00.9	00.10093	00.104971
1.0	00.097178	00.101067

Table 3: Impact of memory parameter α on velocity distribution $\hat{h}(\hat{y}, \hat{t})$ using Stehfest's algorithm

\hat{t}	$\alpha = 0.2$	$\alpha = 0.4$	$\alpha = 0.6$	$\alpha = 0.8$	$\alpha = 1$
0	0.57172	0.437683	0.30004	0.183862	0.105612
0.1	0.571046	0.435936	0.297018	0.179762	0.10085
0.2	0.570333	0.434162	0.293991	0.175701	0.096195
0.3	0.569583	0.432361	0.290961	0.171679	0.091654
0.4	0.568797	0.430536	0.28793	0.167701	0.08723
0.5	0.567977	0.428687	0.284899	0.163769	0.082929
0.6	0.567123	0.426817	0.281871	0.159884	0.078754
0.7	0.566237	0.424925	0.278845	0.156048	0.074709
0.8	0.56532	0.423014	0.275825	0.152264	0.070796
0.9	0.564372	0.421085	0.27281	0.148533	0.067017
1	0.563395	0.419138	0.269803	0.144856	0.063373

Table 4: Impact of distinct parameters on Nusselt number Nu

α	Pr	Nr	\hat{t}	ϕ	Nu
0.6	0.78	0.7	0.1	0.01	2.8190
0.5	0.78	0.6	0.1	0.01	2.53994
0.6	0.78	0.6	0.1	0.01	2.44180
0.6	0.78	0.6	0.1	0.01	3.17093
0.6	0.78	0.6	0.1	0.04	3.23286
0.6	0.78	0.6	0.1	0.04	3.21186

Table 5: Impact of distinct parameters on Sherwood number Sh

α	γ	Sc	\hat{t}	Sh
0.6	0.3	2	0.1	2.29024
0.5	0.3	2	0.1	2.18089
0.5	0.5	2	0.1	2.36571
0.5	0.3	3	0.1	2.80496
0.5	0.3	2	0.2	2.33656

Table 2 displays the changes in velocity against different values of \hat{y} using two algorithms Stehfest's along with Tzou's algorithm for Al_2O_3 nanoparticle. Table 3 evaluates the influences of α on velocity distribution $\hat{h}(\hat{y}, \hat{t})$ using Stehfest's algorithm for the same

nanofluid. Table 4 shows the influence of ϕ , Nr , Pr and \hat{t} on Nusselt number. The Nusselt number decreases for increased value of Nr . Table 5 shows that Sherwood number decreases for greater value of γ .

5. CONCLUSIONS

A scientific examination of MHD fractional nanofluids flow of Brinkman type under the combined effects of heat and mass transfer through the porous media along with four distinct types of spherical shaped nanoparticles is studied in this article. The fluid flow is over an infinite plate placed vertically with thermal radiation and chemical reaction of first order. The velocity slip effects and Newtonian heating are taken into account. A table with thermo-physical properties for nanoparticles is also included. The semi-analytic solutions to velocity function, temperature distribution and concentration field are obtained with the aid of Laplace transformation for fractional calculus. The governing modeled equations with initial as well as boundary conditions are satisfied. The inverse Laplace transformation has been computed numerically with the aid of two algorithms named Stehfest's algorithm [63] and Tzou' algorithm [67] for the validation of our evaluated results. The velocity, temperature and concentration results are developed and shown through graphs related to fractional nanofluid for distinct values of parameter α lying between $0 < \alpha < 1$ and for ordinary nanofluid (when $\alpha = 1$) with related discussion. In all cases, as it was expected, the graphs related to fractional nanofluid tend to superimpose ordinary nanofluid. The concluding remarks are precised as:

- Table 2 shows the validity of two numerical methods.
- The flow of ordinary nanofluid is slower than fractional nanofluid (water based).
- The fluid velocity decreases by raising the value of Brinkman parameter β_1 .
- The fluid velocity of fractional nanofluid as well as ordinary nanofluid is inversely related to volume fraction ϕ of nanoparticles.
- The velocity profile decays with respect to increment in magnetic parameter M .
- The increased values of Gr and Gm results to accelerate the fluid flow of fractional nanofluid.
- An increase in the value of radiation parameter Nr tends to accelerate fluid velocity.
- The parameter of chemical reaction γ as well as Schmidt number Sc shows opposite effect on the concentration field.
- The velocity and temperature distribution for fractional nanofluid are inversely related to Prandtl number Pr .
- The effect of porosity parameter K on velocity profile for fractional nanofluid with respect to M , the magnetic parameter.
- This investigation evaluates that fractional nanofluid have a remarkably different action when we compared with ordinary nanofluid. The references [32] shows the same findings. These findings show that fractional parameter has strong impact over heat transfer phenomena.

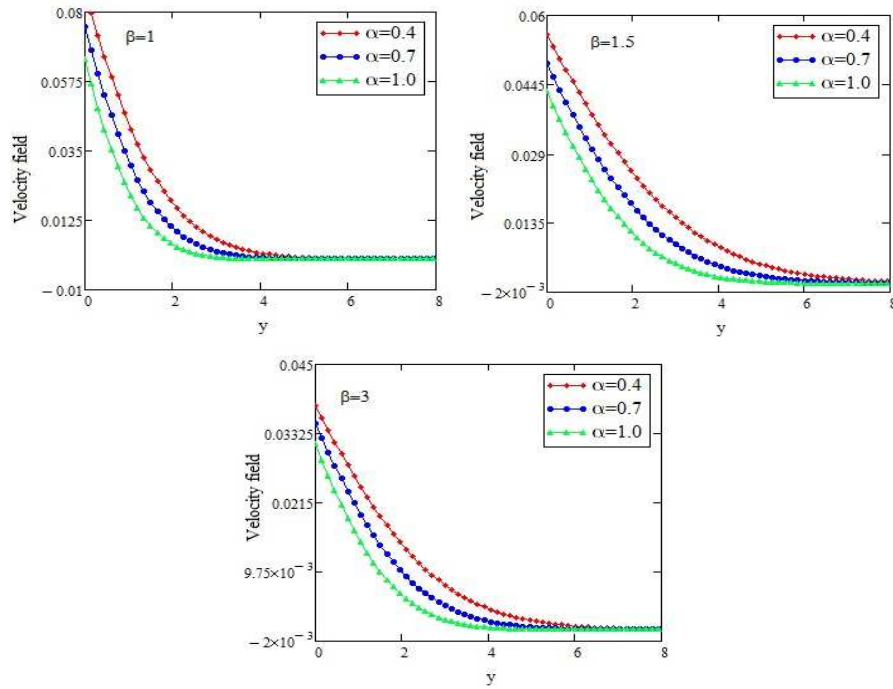


Figure 2: Velocity field representation with various values of fractional parameter and Brinkman parameter $\beta=1, 1.5, 3$.

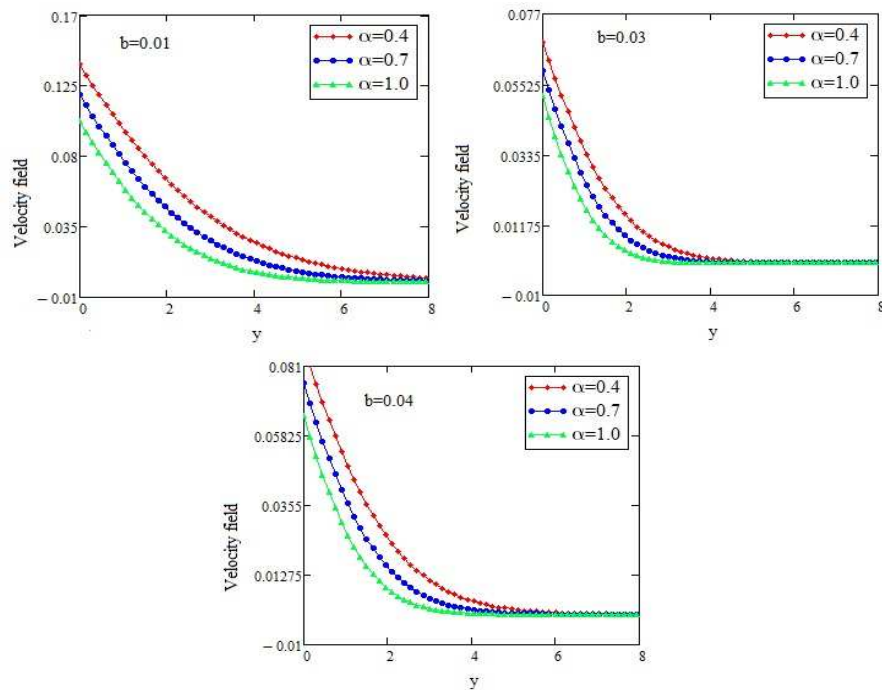


Figure 3: Velocity field representation with various values of α and volume fraction $\phi=b=0.02, 0.03, 0.04$.

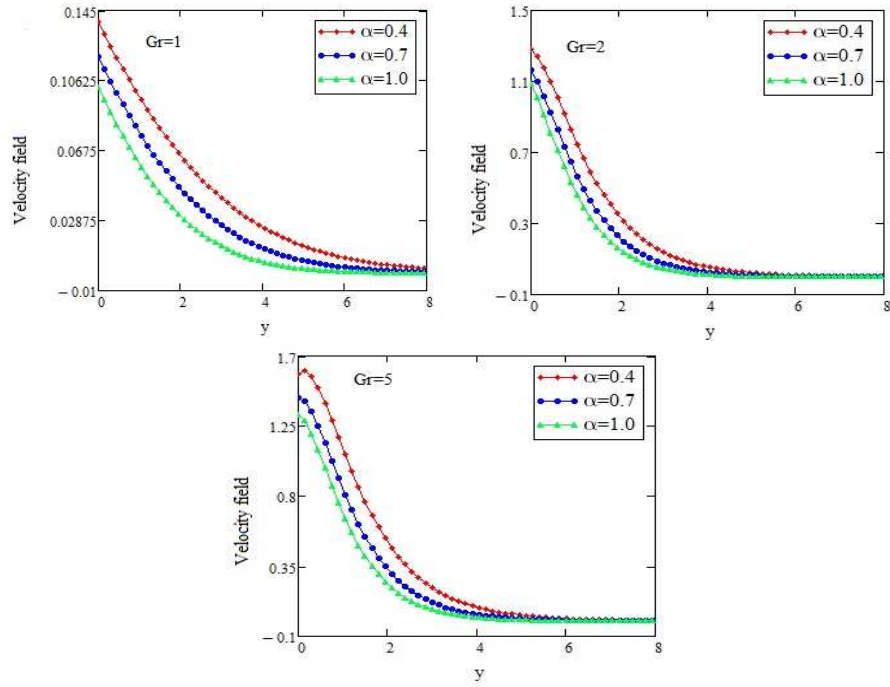


Figure 4: Velocity field representation with distinct values of α and Grashof number $Gr = 1, 2, 5$.

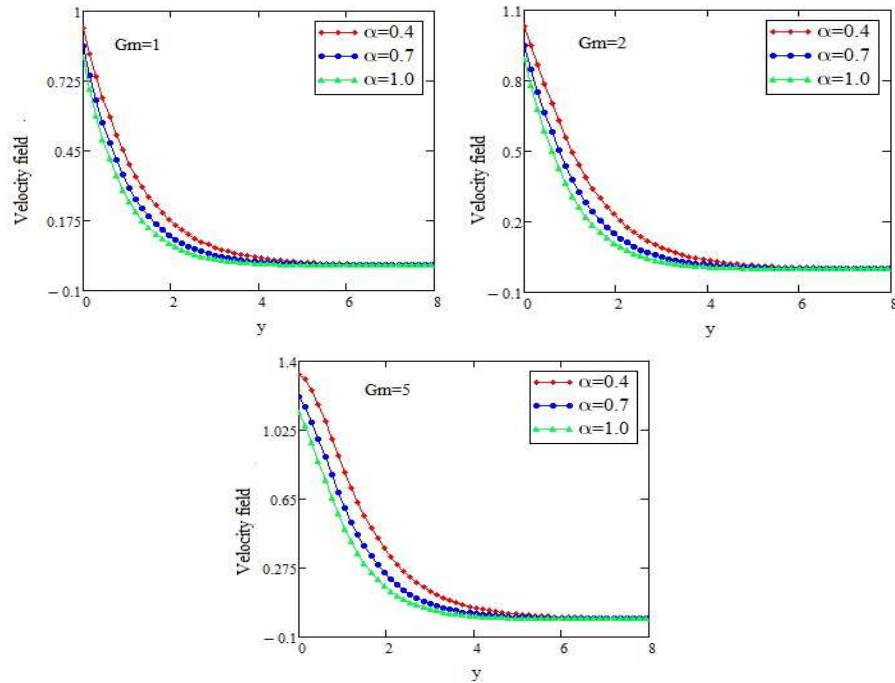


Figure 5: Velocity field representation with distinct values of fractional variable and modified Grashof number $Gm = 1, 2, 5$.

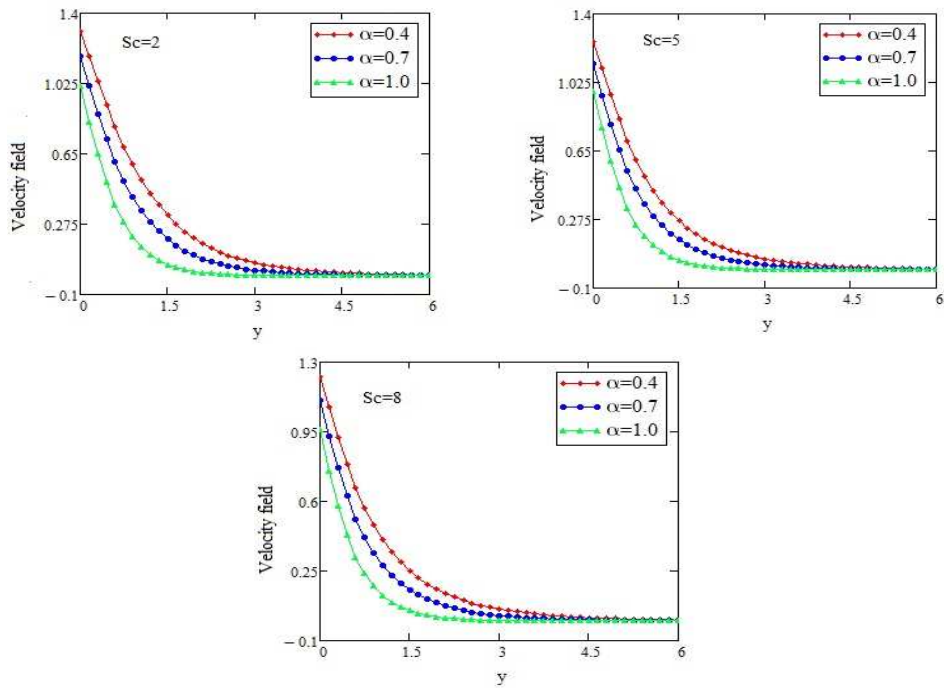


Figure 6: Velocity field representation with various values of fractional parameter and Schmidt number $Sc = 2, 5, 8$.

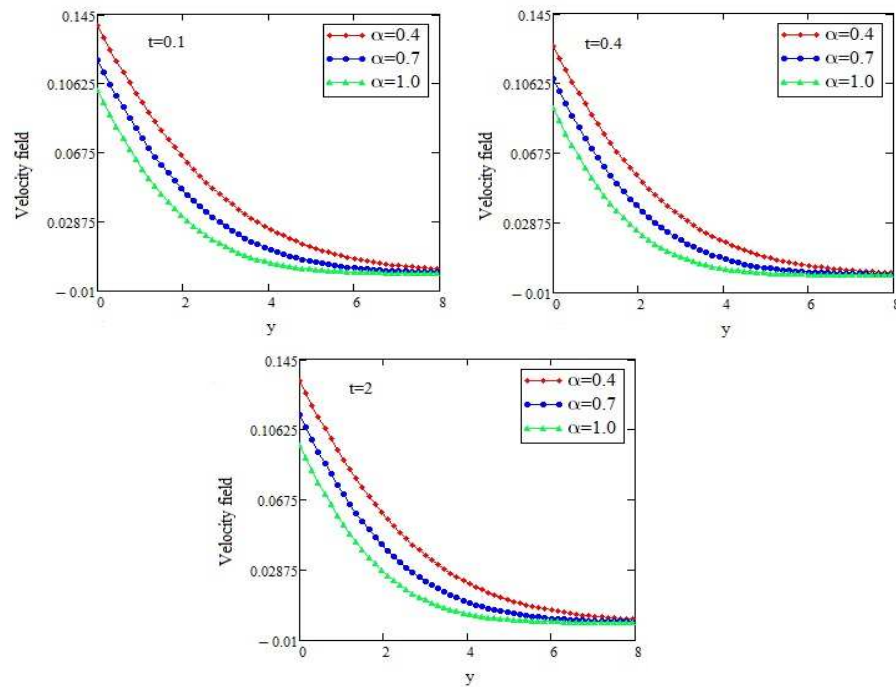


Figure 7: Velocity field representation with various values of fractional parameter and time $t = 0.1, 0.2, 2$.

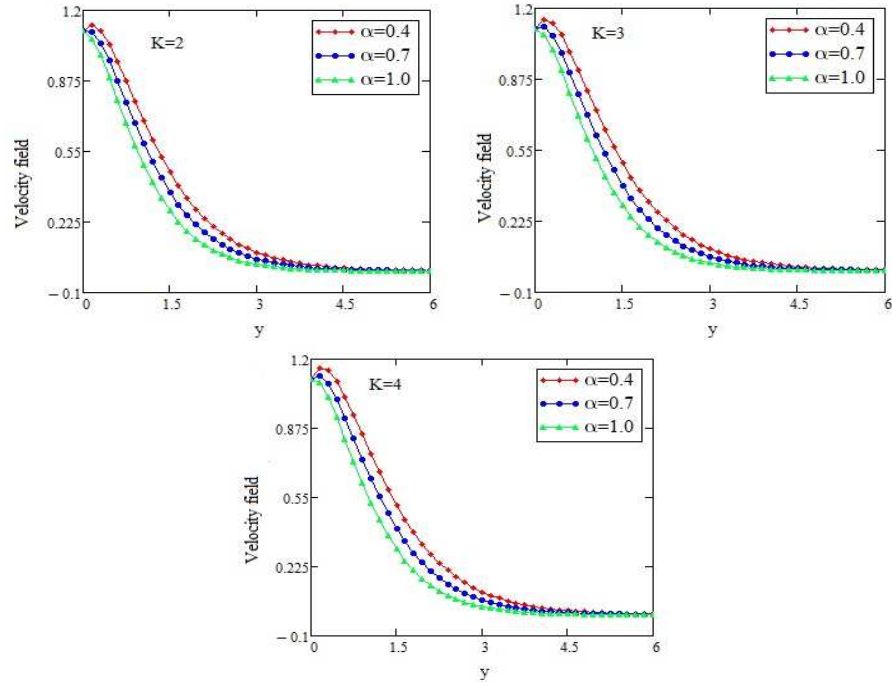


Figure 8: Velocity field representation with various values α and porosity parameter $K = 1, 2, 5$.

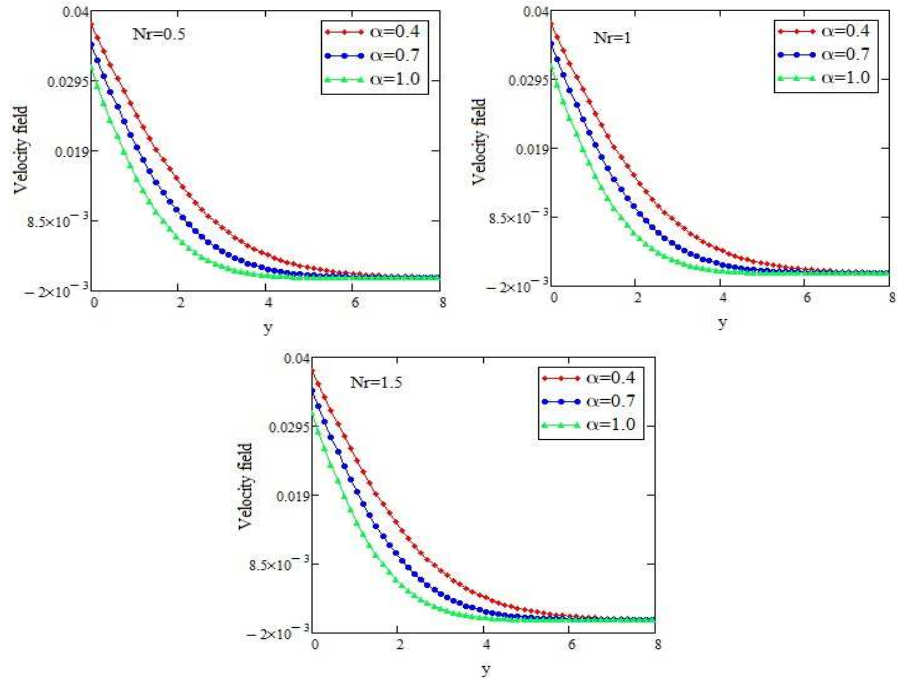


Figure 9: Velocity field representation with distinct values of α and radiation parameter $Nr = 0.5, 1, 1.5$.

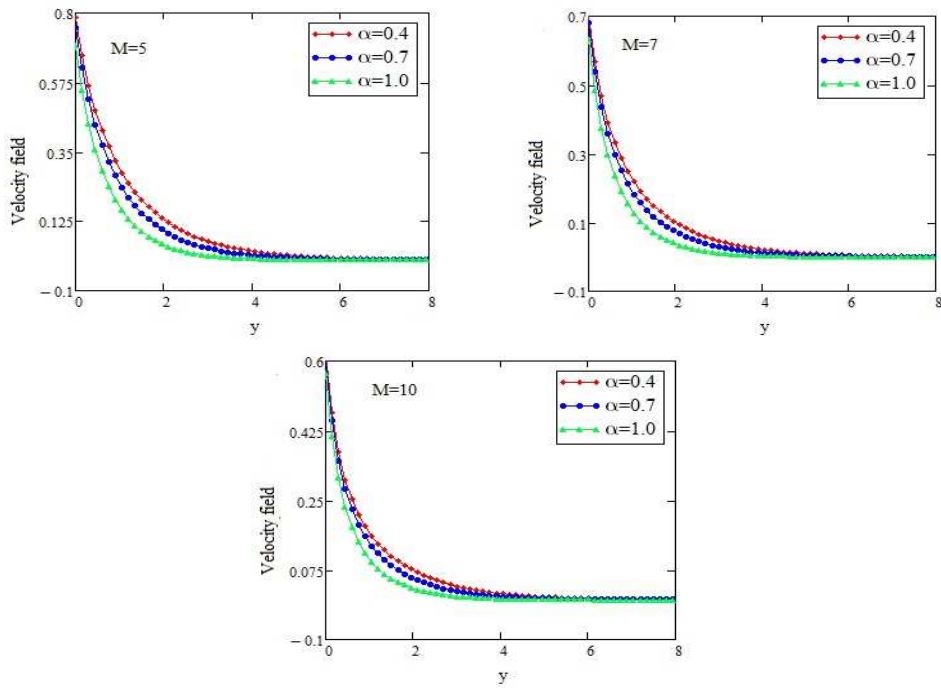


Figure 10: Velocity field representation with various values of α and magnetic parameter $M = 5, 7, 10$.

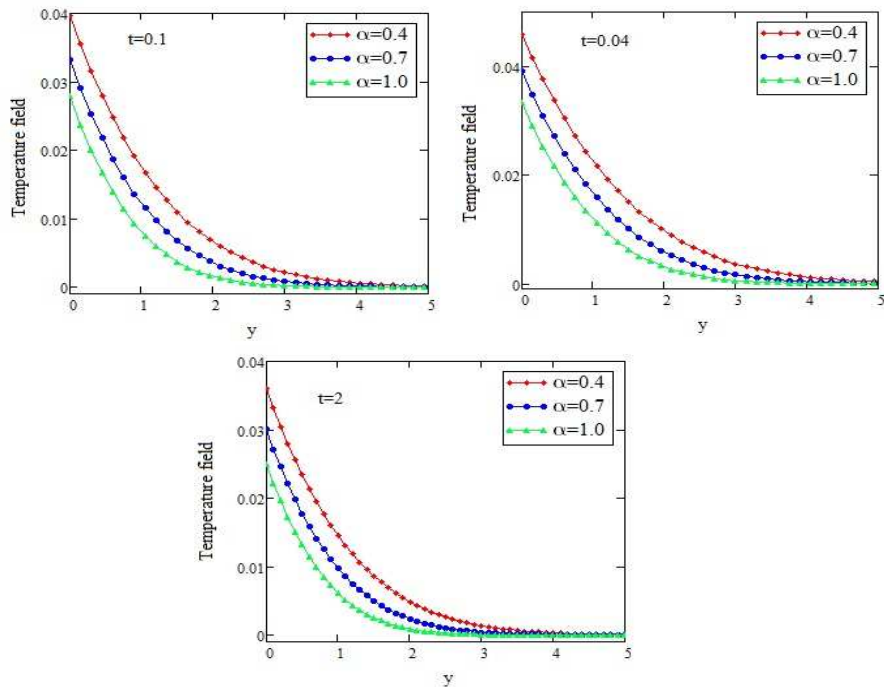


Figure 11: Profiles of temperature field with various values of α and time $\bar{t} = 0.1, 0.04, 2$.

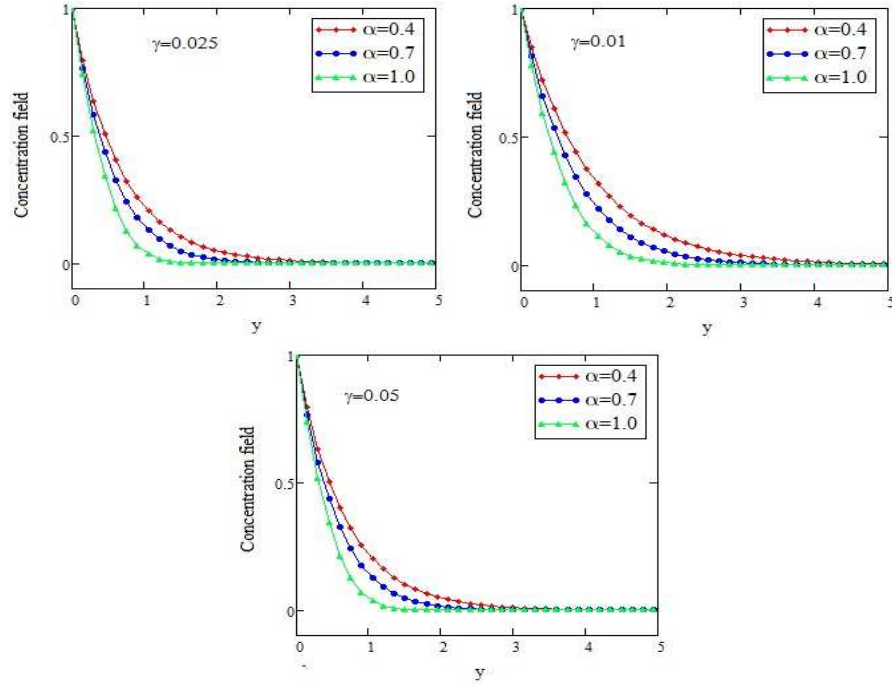


Figure 12: Profiles of concentration field with various values of fractional parameter and $\gamma=0.025, 0.01, 0.05$.

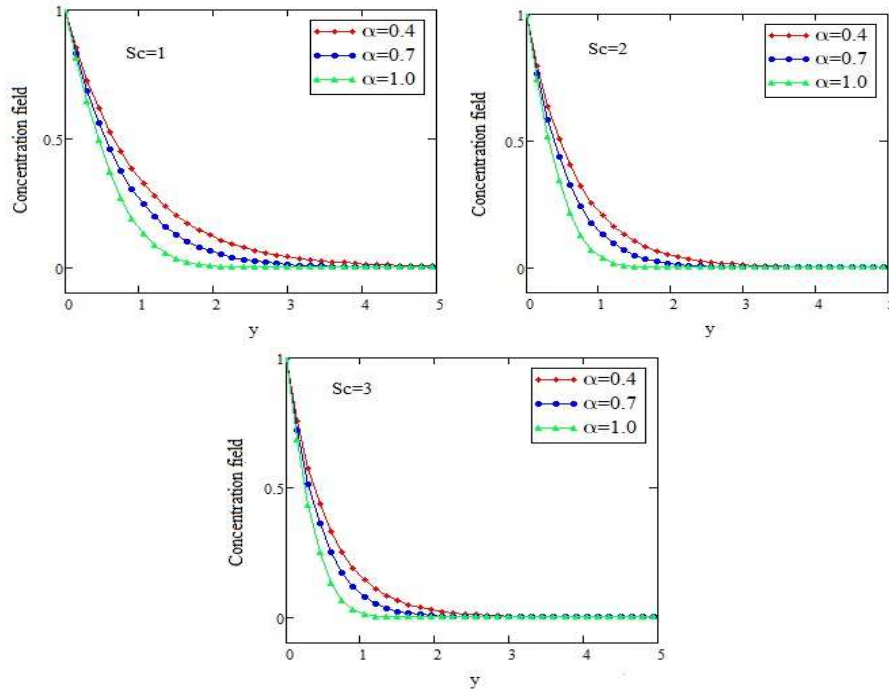


Figure 13: Profiles of concentration field with various values of fractional parameter and Schmidt number $Sc = 1, 2, 3$.

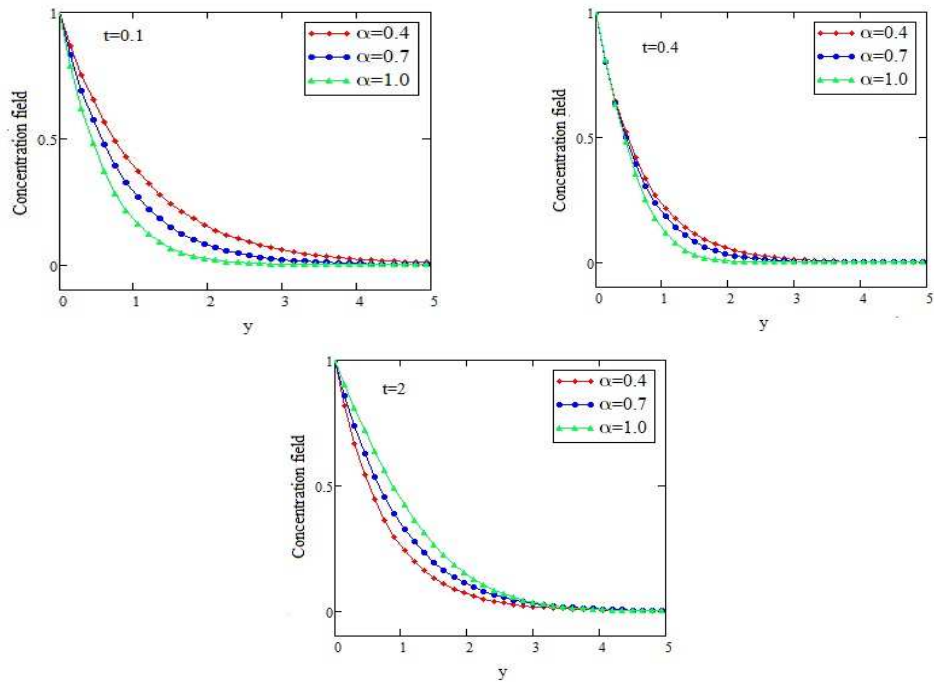


Figure 14: Profiles of concentration field with various values of fractional parameter and time $t = 0.1, 0.4, 2$.

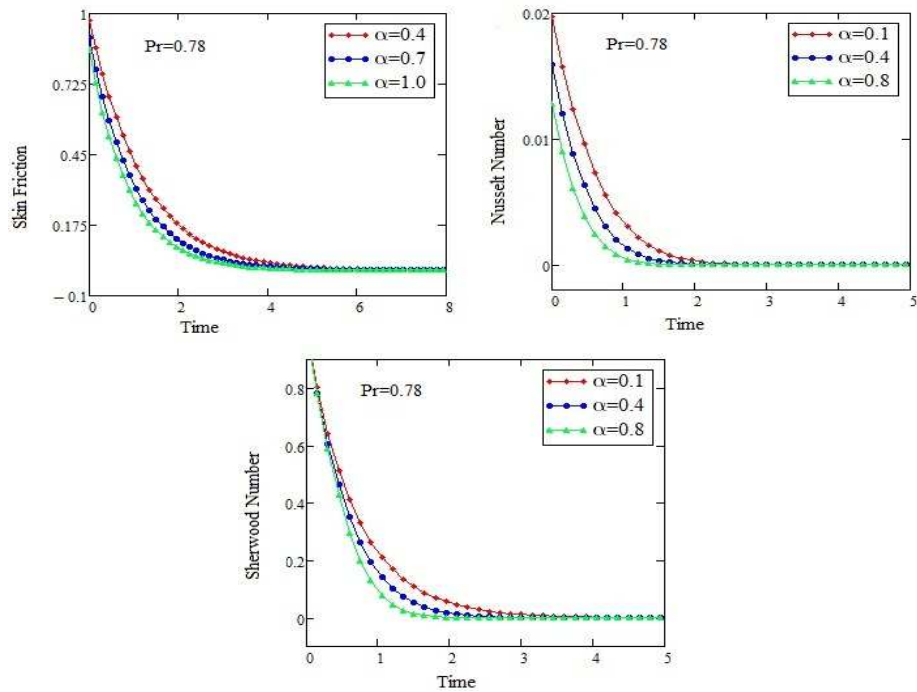


Figure 15: Profiles of skin friction, Nusselt number and Sherwood number with various values of fractional parameter when $Pr=0.78$.

REFERENCES

- [1] A. Aliseda, *Atomization of viscous and non-Newtonian liquids by a coaxial, high-speed gas jet. Experiments and droplet size modeling*, Int. J. Multiphase Flow **34**, No. 2 (2008) 161-175.
- [2] F. Ali, M. Gohar, I. Khan, *MHD flow of water based Brinkman type nanofluid over a vertical plate embedded in a porous medium with variable surface velocity, temperature and concentration*, J. Mol. Liq. **223**, (2016) 412-419.
- [3] N. S. Akbar, S. Nadeem, R. U. Haq, Z. H. Khan, *Radiation effects on MHD stagnation point flow of nano fluid towards a stretching surface with convective boundary condition*, Chin. J. Aeronaut. **26**, No. 6 (2013) 1389-1397.
- [4] M. I. Anwar, I. Khan, S. Sharidan, M. Z. Salleh, *Conjugate effects of heat and mass transfer of nanofluids over a nonlinear stretching sheet*, Int. J. Phys. Sci. **7**, No. 26 (2012) 4081-4092.
- [5] H. C. Brinkman, *On the permeability of media consisting of closely packed porous particles*, Appl. Sci. Res. **1**, No. 1 (1949) 81-86.
- [6] Z. Cao, J. Zhao, Z. Wang, F. Liu, L. Zheng, *MHD flow and heat transfer of fractional Maxwell viscoelastic nanofluid over a moving plate*, J. Mol. Liq. **222**, (2016) 1121-1127.
- [7] A. S. Chethan, G. N. Sekhar, P. G. Siddheshwar, *Flow and heat transfer of an exponential stretching sheet in a viscoelastic liquid with Navier slip boundary condition*, J. Appl. Fluid Mech. **8**, (2015) 223-229.
- [8] S. U. S. Choi, *Enhancing thermal conductivity of fluids with nanoparticles*, ASME Publ. Fed. **231**, (1995) 99-106.
- [9] H. Darcy, *Les fontaines publiques de la ville de Dijon*, Cf. M. Muskat, *The Flow of Homogeneous Fluids Through Porous Media*, (New York 1937), 1856.
- [10] S. Das, S. K. Guchhait, R. N. Jana, *Hall effects on unsteady hydromagnetic flow past an accelerated porous plate in a rotating system*, J. Appl. Fluid Mech. **8**, (2015) 409-417.
- [11] M. E. Davis, R. J. Davis, *Fundamentals of Chemical Reaction Engineering*, Courier Corporation, 2012.
- [12] S. M. M. El-Kabeir, A. M. Rashad, *Boundary-layer heat transfer from a stretching circular cylinder in a nanofluid*, J. Ther. Phys. Ht. Trns. **25**, (2011) 183-186.
- [13] S. M. M. EL-Kabeir, M. Modather, A. M. Rashad, *Effect of thermal radiation on mixed convection flow of a nanofluid about a solid sphere in a saturated porous medium under convective boundary condition*, J. Por. Med. **18**, (2015) 569-584.
- [14] A. Farhad, I. Khan, S. Shafie, *A note on new exact solutions for some unsteady flows of Brinkman-type fluids over a plane wall*, Z. Naturforsch. A **67**, No. 6-7 (2012) 377-380.
- [15] C. Fetecau, C. Fetecau, M. A. Imran, *On Stoke's problem for fluids of Brinkman type*, Math. Rep. **13**, No. 63 (2011) 1526.
- [16] C. Fetecau, D. Vieru, W. Azhar, *Natural convection flow of fractional nanofluids over an isothermal vertical plate with thermal radiation*, J. Appl. Sci. **7**, (2017), doi:10.3390/app7030247.
- [17] D. M. Forrester, J. Huang, V. J. Pinfield, F. Lupp, *Experimental verification of nanofluid shear-wave reconversion in ultrasonic fields*, Nanoscale (2016).
- [18] P. S. Ghoshdastidar, *Heat Transfer*, Oxford University Press, Oxford, UK, 2004.
- [19] A. Graham, G. W. Scott Blair, R. F. J. Withers, *Application of fractional calculus to fluid mechanics*, British J. Phi. Sci. **3** (1961) 265-280.
- [20] F. M. Hady, F. S. Ibrahim, S. M. Abdel-Gaied, M.R. Eid, *Radiation effect on viscous flow of a nanofluid and heat transfer over a nonlinearly stretching sheet*, Nanoscale Res. Lett. **7**, No. 1 (2012) 1-13.
- [21] T. Hayat, Z. Abbas, M. Sajid, *Heat and mass transfer analysis on the flow of a second grade fluid in the presence of chemical reaction*, Phys. Lett. A, **372**, No. 14 (2008) 2400-2408.
- [22] R. U. Haq, S. Nadeem, Z. H. Khan, N. F. M. Noor, *MHD squeezed flow of water functionalized metallic nanoparticles over a sensor surface*, Phys. E. **73**, (2015) 45-53.
- [23] R. U. Haq, N. F. M. Noor, Z. H. Khan, *Numerical simulation of water based magnetite nanoparticles between two parallel disks*, Adv. Powder Technol. (2016).
- [24] R. U. Haq, Z. H. Khan, S. T. Hussain, Z. Hammouch, *Flow and heat transfer analysis of water and ethylene glycol based Cu nanoparticles between two parallel disks with suction/injection effects*, J. Mol. Liq. **221**, (2016) 298-304.
- [25] R. U. Haq, D. Rajotia, N. F. M. Noor, *Thermophysical effects of water driven copper nanoparticles on MHD axisymmetric permeable shrinking sheet: dual-nature study*, Eur. Phys. J. E **39**, No. 3 (2016) 1-12.

- [26] R. U. Haq, F. A. Soomro, T. Mekhaoui, Q. Al-Mdallah, *MHD natural convection flow enclosure in a corrugated cavity filled with a porous medium*, Int. J. Heat, Mass, Trans. **121**, (2018), 1168–1178.
- [27] R. U. Haq, F. A. Soomro, Z. Hammouch, *Heat transfer analysis of CuO-water enclosed in a partially heated rhombus with heated square obstacle*, Int. J. Heat. Mass Trans. **118**, (2018), 773–784.
- [28] A. A. Hill, *Convection induced by the selective absorption of radiation for the Brinkman model*, Contin. Mech. Thermodyn. **16**, No. 1-2 (2004) 43-52.
- [29] S. T. Hussain, Z. H. Khan, S. Nadeem, *Water driven flow of carbon nanotubes in a rotating channel*, J. Mol. Liq. **214**, (2016) 136-144.
- [30] S. A. Hussain, G. Ali, S. I. A. Shah, S. Muhammad and M. Ishaq, *Bioconvection Model for Magneto Hydrodynamics Squeezing Nanofluid Flow with Heat and Mass Transfer Between Two Parallel Plates Containing Gyrotactic Microorganisms Under the Influence of Thermal Radiations*, Punjab Univ. J. Math. **51**, No. 4 (2019) 13-36.
- [31] M. Ishaq, G. Ali, S. I. A. Shah, Z. Shah, S. R. Muhammad and S. A. Hussain, *Nanofluid Film Flow of Eyring Powell Fluid with Magneto Hydrodynamic Effect on Unsteady Porous Stretching Sheet*, Punjab Univ. J. Math. **51**, No. 3 (2019) 147-169.
- [32] R. Kandasamy, R. Mohamad, M. Ismoen, *Impact of chemical reaction on Cu, Al₂O₃, SWCNTs-nano fluid flow under slip conditions*, J. Eng. Sci. Tech. **19**, (2016) 700–709.
- [33] A. Khalid, I. Khan, S. Shafie, *Exact solutions for free convection flow of nanofluids with ramped wall temperature*, Eur. Phys. J. Plus **130**, No. 4 (2015) 1-14.
- [34] I. Khan, *Shape effects of MoS₂ nano particles on MHD slip flow of molbdenum disulphide nano fluid in a porous medium*, J. Mol. Liq. **233**, (2017) 442–451.
- [35] P. Loganathan, P. Nirmal Chand, P. Ganesan, *Radiation effects on an unsteady natural convective flow of a nanofluid past an infinite vertical plate*, Nano **8**, No. 1 (2013) DOI: 10.1142/S179329201350001X.
- [36] Lissant, J. Kenneth, *Non-Newtonian Pharmaceutical Compositions*, U. S. Patent No. 4, 040, 857. Aug. 9, 1977.
- [37] C. Lin, L. E. Payne, *Structural stability for a Brinkman fluid*, Math. Meths. Appl. Sci. **30**, No. 5 (2007) 567-578.
- [38] J. H. Markin, *Natural convection boundary layer flow on a vertical surface with Newtonian heating*, Int. J. heat fluid flow, **15**, (1994) 392-398.
- [39] K. B. Migler, H. Hervet, L. Leger, *Slip transition of a polymer melt under shear stress*, Phys. Rev. Lett. **70**, (1993) 287-290.
- [40] M. Mooney, *Explicit formulas for slip and fluidity*, J. Rhe. **2**, (1931) 210-222.
- [41] P. V. S. N. Murthy, Ch. RamReddy, A. J. Chamka, A. M. Rashad, *Magnetic effect on thermally stratified nanofluid saturated non-Darcy porous medium under convective boundary condition*, Int. Comm. Heat, Mass, Tran. **47**, (2013) 41–48.
- [42] M. Narahari, *Newtonian heating and mass transfer on free convection flow past an accelerated plate in the presence of thermal radiation*, AIP, Conf. Proc. **1482**, (2012), 340-346.
- [43] M. Narahari, B. K. Dutta, *Effect of thermal radiation and mass diffusion on free convection plate near a vertical plate with Newtonian heating*, Chem. Eng. Commun. **199**, (2012) 628-643.
- [44] M. Navier, *The effect of slip condition on unsteady MHD oscillatory flow of a viscous fluid in a planar channel*, Mem. Acad. Sci. Inst. France, **1**, (1823) 414-416.
- [45] G. Neale, W. Nader, *Practical significance of Brinkman's extension of Darcy's law: coupled parallel flows within a channel and a bounding porous medium*, Can. J. Chem. Eng. **52**, No. 4 (1974) 475-478.
- [46] M. Pan, L. Zheng, F. Liu, X. Zhang, *Modeling heat transport in nanofluids with stagnation point flow using fractional calculus*, Appl. Math. Model. **40**, (2016) 8974-8984.
- [47] A. Purusothaman, N. Nithyadevi, H. F. Oztop, V. Divya, K. Al. Saleem, *Three dimensional numerical analysis of natural convection cooling with an array of discrete heaters embedded in nanofluid filled enclosure*, Advan. Powd. Tech. **27**, (2016) 268-280.
- [48] A. Purusothaman, H. F. Oztop, N. Nithyadevi, Nidal H. Abu. Hamdeh, *3D natural convection in a cubical cavity with a thermally active heater under the presence of an external magnetic field*, Comp. Fluids, **128**, (2016) 30-40.
- [49] A. Purusothaman, A. Bairi, N. Nithyadevi, *3D natural convection on a horizontal and vertically thermally active plate in a closed cubical cavity*, Int. J. Num. Meth. Heat Fluid Flow, **26**, (2015) 2528-2542.

- [50] A. Purusothaman, V. Divya, N. Nithyadevi, H. F. Oztop, *An analysis on free convection cooling of a 3×3 heater array in rectangular enclosure using Cu-EG-water nanofluid*, J. Appl. Fluid Mech. **9**,(2016) 3147-3157.
- [51] A. Purusothaman, *Investigation of natural convection heat transfer performance of the QFN-PCB electronic module by using nanofluid for power electronics cooling applications*, Advanc. Powd. Tech, **29**, (2018) 996-1004.
- [52] A. Purusothaman, R. Chandra Guru Sekar, K. Murugesan, *Magnetic field and vibration effects on the onset of thermal convection in a grade fluid permeated anisotropic porous module*, Therm. Sci. Eng. Progr. **10**, (2019) 138-146.
- [53] A. Purusothaman, E. H. Malekshah, *Lattice Boltzman modeling of MHD free convection of nanofluid in a V-shaped microelectronic module*, Ther. Sci. Eng. Prog. **10**, (2019) 186-197.
- [54] I. J. Rao, K. R. Rajagopal, *The effect of the slip boundary condition on the flow of fluids in a channel*, Act. Mech. **135** (1999) 113-126.
- [55] A. Rahimi , A. Kasaeipoor , E. H. Malekshah , M. M. Rashidi , A. Purusothaman, *Lattice Boltzman simulation of 3D natural convection in a cuboid filled with KKL-model predicted nanofluid using Dual-MRT model*, Int. J. Num. Meth. Heat Fluid Flow, **9**,(2019) 365-387.
- [56] M. Ramzan, *MHD three dimensional flow of couple stress field with Newtonian heating*, Eur. Phy. J. Plus, **5**, (2013) 128.
- [57] A. M. Rashad, A. J. Chamka, M. M. M. Abdou, *Mixed Convection flow of non-Newtonian fluid from vertical surface saturated in a porous medium filled with a nanofluid*, J. App. Fluid Mech. **6** (2013) 301–309.
- [58] A. M. Rashad, A. J. Chamka, M. Modather, *Mixed convection boundary layer flow past a horizontal circular cylinder embedded in a porous medium filled with a nanofluid under convective boundary condition*, J. Comp. Fluids, **86** (2013) 380–388.
- [59] A. M. Rashad, A. J. Chamkha, S. M. M. El-Kabeir, *Effect of chemical reaction on heat and mass transfer by mixed convection flow about a sphere in a saturated porous media*, Int. J. Numer. Methods Heat Fluid Flow, **21**, No. 4 (2011) 418-433.
- [60] A. M. Rashad, *Impact of thermal radiation on MHD slip flow of a Ferrofluid over a nonisothermal wedge*, J. Magn. Mag. Mat. **422**, (2017) 25–31.
- [61] N. Raza, *Unsteady Rotational Flow of a Second Grade Fluid with Non-Integer Caputo Time Fractional Derivative*, Punjab Univ. J. Math. **49**, No. 3 (2017) 15-25.
- [62] S. U. Rehman, R. U. Haq, Z. H. Khan, C. Lee, *Entropy generation analysis for non-Newtonian nanofluid with zero normal flux of nanoparticles at the stretching surface*, J. Taiwan Inst. Chem. Eng. **63**, (2016) 226-235.
- [63] H. Stehfest, *Algorithm 368: Numerical inversion of Laplace transforms*, Commun. ACM, **13**, (1970) 47–49.
- [64] G. S. Seth, R. Nandkeolyar, M. S. Ansari, *Effects of thermal radiation and rotation on unsteady hydromagnetic free convection flow past an impulsively moving vertical plate with ramped temperature in a porous medium*, J. Appl. Fluid Mech. **6**, No. 1 (2013) 27-38.
- [65] M. Sheikholeslami, D. D. Ganji, *Three dimensional heat and mass transfer in a rotating system using nanofluid*, Powd. Technol. **253**, (2014) 789-796.
- [66] R. I. Tanner, *Partial wall slip in polymer flow*, Inds. Eng. Chem. Res. **33**, (1994) 2434-2436.
- [67] D. Y. Tzou, *Macro to Microscale Heat Transfer: The Lagging Behaviour* Taylor and Francis, Washington, (1997).
- [68] M. Usman, F. A. Soomro, R. U. Haq, W. Wang, O. Defterli, *Thermal and velocity slip effects on Casson nanofluid flow over an inclined permeable stretching cylinder via collocation method*, Int. J. Heat. Mass. Trans. **122**, (2018) 1255–1263.
- [69] M. Usman, T. Zubair, M. Hamid, R. U. Haq, W. Wang, *Wavelets solution of MHD 3-D fluid flow in the presence of slip and thermal radiation effects*, Phy. Fluids, **30**, (2018) 023104.
- [70] H. A. Wahab, H. Zeb, S. Bhatti, M. Gulistan and S. Ahmad, *A Numerical Approach of Slip Conditions Effect on Nanofluid Flow over a Stretching Sheet under Heating Joule Effect*, Punjab Univ. J. Math. **51**, No. 4 (2019) 79-95.
- [71] E. R. E. L Zahar, A. M. Rashad, A. M. Gelany, *Studying high suction effect on boundary-layer flow of a nanofluid on permeable surface via singular perturbation technique*, J. Comp. The. Nano Sci. **12**, (2015) 4828–4836.

- [72] M. N. Zakaria, A. Hussanan, I. Khan, S. Shafie, *The effects of radiation on free convection flow with ramped wall temperature in Brinkman type fluid*, J. Technol. **62**, No.3 (2013) 33-39.